Soft Matter

PAPER

View Article Online
View Journal

Cite this: DOI: 10.1039/d0sm00833h

Double cross-linked supramolecular hydrogels with tunable properties based on host–guest interactions†

Yunjiao Che,[ab] Jens Gaitzsch,[a] Nikolai Liubimtsev,[ab] Stefan Zschoche,[a] Tim Bauer,[c] Dietmar Appelhans *[a] and Brigitte Voit *[ab]

We report a novel double cross-linked hydrogel system based on polyacrylamide and poly(2-methyl-2-oxazoline) (PMOXA) network chains, as well as on supramolecular host–guest interactions with on-demand tailored mechanical properties. Well-defined vinyl-bearing PMOXA macromonomers, functionalized with either β-cyclodextrin units (β-CD–PMOXA) or adamantane units (Ada–PMOXA), were synthesized and confirmed using ^{1}H NMR, MALDI-TOF-MS and GPC measurements. The complexation between adamantane and β-CD modified macromonomers in solution towards bismacromonomers was confirmed by 2D NOESY NMR and DLS. After introducing these bismacromonomers into the polyacrylamide hydrogel, the supramolecular non-covalent Ada/β-CD bond was responsible for the presence of PMOXA network chains to form a dense network. Once the interactions broke, the PMOXA chains no longer contributed to the network, but became dangling graft side chains in a predominated polyacrylamide network. Their dissociative nature influenced the physical properties, including the swelling behavior and mechanics of the final hydrogel. Rheological experiments proved that the E-modulus of the network was significantly increased by the supramolecular host–guest interactions. Tuning the lengths of PMOXA network chains even allowed the modification of the changes in mechanical strength, also through the addition of free β-CD. The tunable properties of the double cross-linked supramolecular hydrogel proved their unique strength for future applications.

Received 8th May 2020,
Accepted 11th June 2020

DOI: 10.1039/d0sm00833h

rsc.li/soft-matter-journal

Introduction

Hydrogels are three-dimensional (3D) networks of cross-linked hydrophilic polymers that can retain and absorb considerable quantities of water. Due to their highly attractive features, such as water adsorption, biodegradability and environmental responsiveness, hydrogels are desirable for numerous applications, for example, in drug delivery systems,[1,2] tissue engineering,[3] biosensors,[4,5] and shape memory materials.[6,7] Generally speaking, the approaches for constructing hydrogels are classified into two categories: through covalent cross-linking and non-covalent cross-linking. In comparison to covalent bonds, hydrogels bearing non-covalent bonds possess the advantages of versatility and tunability. Supramolecular hydrogels driven by dynamic non-covalent intermolecular forces, such as hydrogen bonding,[8,9] π–π stacking,[10] ionic,[11,12] as well as hydrophobic interactions,[13] have created unprecedented functions and have become a series of promising materials in the field of polymer chemistry. Among the numerous intermolecular forces, host–guest interactions have drawn considerable attention for the design of dynamic hydrophilic functional materials in recent years.[14–16]

Host–guest complexes are constructed of two or more chemical units, in which one chemical entity (the "guest") is inserted into the cavity of another chemical entity (the "host") driven by hydrophobic and van der Waals interactions.[17] Due to their unique responsive and dynamic properties, a large number of macrocycles have been established as hosts in the last few decades, *e.g.*, cavitands,[18] crown ethers,[19] calix[*n*]arenes,[20] cucurbit[*n*]urils[21] and porphyrins.[22] In particular, cyclodextrins (CDs) have become one of the most powerful candidates. Since CDs exhibit a hollow cylindrical structure with a hydrophobic interior cavity, they have a strong host–guest affinity with a variety of lipophilic compounds, forming inclusion complexes in a solvent.[23,24] Numerous supramolecular hydrogels based on host–guest interactions between CDs with various guest

[a] *Leibniz-Institut für Polymerforschung Dresden e.V., Hohe Straße 6, 01069 Dresden, Germany. E-mail: voit@ipfdd.de, applhans@ipfdd.de*
[b] *Technische Universität Dresden, Faculty of Chemistry and Food Chemistry, Organic Chemistry of Polymers, 01069 Dresden, Germany*
[c] *Technische Universität Dresden, Faculty of Chemistry and Food Chemistry, Chair of Macromolecular Chemistry, 01069 Dresden, Germany*

† Electronic supplementary information (ESI) available. See DOI: 10.1039/d0sm00833h

molecules such as adamantane,[25] azobenzene,[26] ferrocene[27] and anthraquinone[28] have been reported. As one of the most investigated guest molecules, adamantane derivatives (Ada) have attracted much attention. Benefiting from specific structural features, adamantane can form a 1:1 inclusion complex with β-CD with a high association constant at 10^4–10^5 M^{-1}.[17,23,29] Thus, the inclusion complexes between adamantane and β-CD have been frequently exploited for forming supramolecular hydrogels bearing shape-memory,[30,31] self-healing[32,33] and injectable properties.[34] For instance, Harada and co-workers[35] reported a self-assembling supramolecular hydrogel consisting of adamantane- and β-CD acrylamide monomers. The resulting hydrogels showed high stretchability up to 990% and a profound shape recovery property, indicating that the host–guest interactions played a vital role in controlling the properties of supramolecular hydrogels. Burdick *et al.*[36] reported a self-healing double-network (DN) hydrogel based on the rapid association of adamantane- and β-CD functionalized hyaluronic acid (HA). The one-pot prepared supramolecular-covalent hydrogels presented unique properties for load-bearing, injectability, and cytocompatibility. More recently, Mao and co-workers[37] constructed novel "three-arm" Ada/β-CD supramolecular hydrogels. The host–guest complex endowed the hydrogel with strong fatigue/slicing resistance and it was also proven to have reversible mechanical properties. The self-healing property enabled the hydrogel to be a promising biomaterial for soft-tissue repair. While Ada/β-CD supramolecular hydrogels have been developed for numerous applications, almost no systematic investigations of the network structure and its determining inputs are carried out. Moreover, a simple and effective synthetic strategy for the formation of a tunable network is still lacking. Considering the aforementioned reasons, there is an imperative need to construct well-defined hydrogels exploring the relationship between the host–guest efficiency and the network structure. Following our work on double cross-linked hydrogels based on reversible disulfide cross-linkers,[38] we transferred our knowledge to the reversible Ada/β-CD interactions. Since breaking and reforming disulfide bonds had a profound effect on the swelling and mechanical properties of the gel, similar effects were expected with supramolecular forces. Moreover, supramolecular forces could be broken independent of the redox potential of the surrounding solution, which broadens the potential applications.

We herein report a novel hydrogel consisting of two types of cross-linkers, a bisacrylamide and a PMOXA bismacromonomer equipped with Ada/β-CD host–guest interactions (Fig. 1). After polymerization, the PMOXA chains of the bismacromonomer contribute as network chains to the hydrogel, since they are held together by the host–guest interactions. Varying the PMOXA chain length and the option for bond breakage and bonding of the Ada/β-CD host–guest interactions in the hydrogel network under chemical and physical stimuli promises greater insight into the network structure. It also opens the possibility for additional functionalization and release cargo within the network for various oncoming applications.

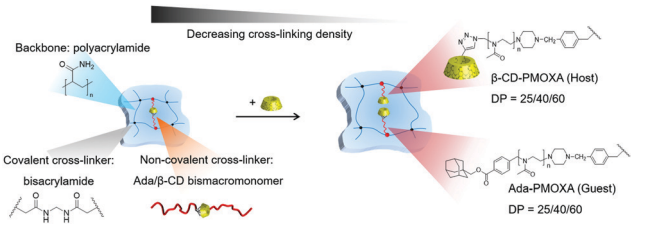

Fig. 1 Double cross-linked supramolecular hydrogels formed by the host–guest interaction between β-CD and adamantane, and the chemical structures of the compounds used.

To accomplish the host–guest-functionalized bismacromonomer, poly(2-methyl-2-oxazoline) (PMOXA) was used as the basic polymer. As a hydrophilic, non-toxic and biocompatible polymer, PMOXA is widely used in drug delivery systems and even in the food industry.[39–42] Moreover, PMOXA can be bi-functionalized in the α- and ω-positions using various functional initiators and terminating agents. This always results in the development of a well-defined polymer through controlled polymerization.[43,44] For this, adamantane- and β-cyclodextrin functionalized PMOXA macromonomers (Ada–PMOXA$_n$, CD–PMOXA$_n$, with n = 25, 40 and 60 and a vinylic monomer function) were synthesized *via* living cationic ring–opening polymerization (LCROP). The formation of well-defined polymer architectures was evaluated by ^{1}H NMR, MALDI-TOF-MS and GPC analyses. The rapid self-assembly of the host–guest-functionalized bismacromonomer was confirmed by 2D NOESY NMR and DLS.

The double cross-linked supramolecular hydrogel was prepared from the monomer acrylamide and the cross-linkers, *N*,*N*′-methylenebis(acrylamide) (BIS) and the PMOXA bismacromonomer, *via* free radical polymerization (FRP) in water. Breaking the host–guest interactions within the PMOXA network chains by introducing a competitive unit should transform the hydrogel into an acrylamide hydrogel with graft PMOXA side chains (= graft dangling side chains) (Fig. 1). Probing the mechanical properties of the network was then used to measure the influence of this change on the overall structure and on the elastic behavior of the hydrogel. Different PMOXA chain lengths even allowed the fine-tuning of the changes in these properties, thus allowing us to pinpoint them to tailor-made hydrogels with tunable mechanics. This novel design offers insights into controlling the overall structure of a hydrogel.

Materials and methods

Materials

Propargyl *p*-toluenesulfonate (*p*-OTs, Sigma-Aldrich, 95%) and methyl trifluoromethanesulfonate (MeOTf, Sigma-Aldrich, 98%) were purified by distillation and stored under an argon atmosphere prior to use. 2-Methyl-2-oxazoline (MOXA, Sigma-Aldrich, 98%) was refluxed over CaH_2 and distilled under argon before use. All other chemicals and solvents were purchased from Sigma-Aldrich, VWR Chemicals or Acros, and used as

received without further purification. A complete list of substances can be found in the ESI.†

Synthesis

Initiator I-1. I-1 was synthesized as previously reported.[45] In brief, under an argon atmosphere, 1-adamantanemethanol (2 g, 12.04 mmol, 1 eq.) was dissolved in dichloromethane (60 mL), followed by adding dry Et_3N (1.22 g, 12.02 mmol, 1 eq.). After adding *p*-bromomethylbenzoyl bromide (4.78 g, 17.20 mmol, 1.4 eq.) dropwise into the solution at 0 °C, the solution was stirred under reflux for 1.5 h. Then the solvent was removed under vacuum and the crude product was purified twice by column chromatography first with dichloromethane/hexane = 2 : 1 (vol/vol) and then with ethyl acetate/hexane = 1 : 8 (vol/vol) as eluents, thus yielding **I-1** as a colorless solid (3.27 g, 75%).

^{1}H NMR ($CDCl_3$, signals assigned in Fig. S1, ESI†): δ (ppm) = 8.10 (d, 2H, H_e), 7.48 (d, 2H, H_f), 4.52 (s, 2H, H_g), 3.92 (s, 2H, H_d), 2.04 (m, 3H, H_b), 1.76 and 1.71 (s, 6H, H_a), 1.65 (d, 6H, H_c).

Vinylating agent *N*-(4-vinylbenzyl)piperazine (4-VBP) (V-1). V-1 was synthesized as previously reported.[46] In brief, piperazine (19.8 g, 0.23 mol, 10 eq.) and 4-vinylbenzyl chloride (2.3 g, 0.02 mol, 1 eq.) were dissolved in anhydrous chloroform (125 mL) at 0 °C, followed by adding trace amounts of 2,6-di-*tert*-butyl-4-methylphenol (BHT) as a stabilizer. The solution was stirred at room temperature (RT) overnight. After the organic solution was extracted with 100 mL water 5 times and dried over Na_2SO_4, the solvent was removed under vacuum, thus yielding **V-1** as a yellow oil (2.66 g, 88%).

^{1}H NMR ($CDCl_3$, signals assigned in Fig. S1, ESI†): δ (ppm) = 7.28 (AA′XX′, 4H, $H_{n,m}$), 6.72, 5.74, 5.23 (ABX, 3H, CH═CH_2, $H_{o,p}$), 3.49 (s, 2H, H_k), 2.92 (m, 4H, H_j), 2.44 (m, 4H, H_j), 1.75 (s, 1 H, H_t).

The following describes polymer synthesis for 40 repeating units. Shorter polymers (around 26 repeating units) were synthesized with 25 eq. of MOXA and longer polymers (around 60 repeating units) were synthesized with 55 eq. of MOXA. The longer polymers were named accordingly by amending the number of repeating units of PMOXA (see the main text).

Adamantane-PMOXA$_{42}$-VBP (Ada-42). In a glove box or under an argon atmosphere, the adamantane-initiator (**I-1**, 0.1066 g, 0.29 mmol, 1 eq.) was dissolved in dry acetonitrile (3 mL), followed by adding fresh distilled 2-methyl-2-oxazoline (1 g, 11.75 mmol, 40 eq.). Then the solution was stirred at 80 °C for 8 h. After cooling to RT, the vinylating agent **V-1** (0.29 g, 1.45 mmol, 5 eq.) was added and the solution was stirred for 24 h. Afterwards, approx. 0.25 g anhydrous K_2CO_3 was added and the mixture was stirred for further 24 h. After the resulting suspension was centrifuged, the organic phase was first filtered through a 20 μm PTFE syringe filter and removed under vacuum. The resulting solid was diluted with methanol (2 mL) and precipitated twice in dry diethyl ether (150 mL) at 0 °C. The crude product was obtained under vacuum. To remove the excess vinylating agent, the solid was dialyzed against methanol with cellulose membranes of MWCO = 1000 (Carl Roth GmbH, Germany) for 3 days. The pure polymer **Ada-42** was obtained as a colorless powder after freeze-drying (Alpha 1-2 LDplus, Martin Christ, Germany) under vacuum (511 mg, 48%).

^{1}H NMR ($CDCl_3$, signals assigned in Fig. 2a and Fig. S2, ESI†): δ (ppm) = 8.03 (H_e), 7.28–7.15 (H_f, H_m, H_n, partly overlap with $CDCl_3$), 6.65 (H_o), 5.65 and 5.13 (H_p), 4.55 (H_g), 3.70 (H_d), 3.60–3.20 (H_h and H_k), 2.50–2.30 (H_j), 2.12–1.97 (H_b and H_i), 1.72–1.58 (H_a), 1.55 (H_c).

Alkynyl-PMOXA$_{41}$-VBP (Alk-41). Under an argon atmosphere, propargyl *p*-toluenesulfonate (51 μL, 0.29 mmol, 1 eq.) was dissolved in dry acetonitrile (3 mL), followed by adding 2-methyl-2-oxazoline (1 g, 11.75 mmol, 40 eq.). The polymerization time was 3.5 h at 70 °C, and the termination and purification were the same as described for **Ada-42**. The macromonomer **Alk-41** was obtained as a colorless powder (353 mg, 33%).

^{1}H NMR ($CDCl_3$, signals assigned in Fig. 2b and Fig. S3, ESI†): δ (ppm) = 7.32–7.15 (H_m, H_n, partly overlap with $CDCl_3$), 6.63 (H_o), 5.65 and 5.15 (H_p), 4.24–3.95 (H_g), 3.65–3.20 (H_g and H_k), 2.50–2.30 (H_j and H_q), 2.13–1.95 (H_i).

Cyclodextrine-PMOXA$_{41}$-VBP (CD-41). Alkynyl-macromonomer **Alk-41** (250 mg, 0.069 mmol, 1 eq.) and 6-monoazido-6-monodeoxy-β-cyclodextrin (95.91 mg, 0.083 mmol, 1.2 eq., Cyclodextrin-Shop, the Netherlands) were dissolved in 2 mL of *N*,*N*-dimethylformamide (DMF). After the reaction mixture was degassed with argon for 10 min, sodium ascorbate (1.77 mg, 0.009 mmol, 0.13 eq.) in 100 μL Milli-Q water was added, followed by adding $CuSO_4{\cdot}5H_2O$ (1.72 mg, 0.0069 mmol, 0.1 eq.) in 100 μL water. The solution was stirred at RT for 3 days. Afterwards the solvent was removed under vacuum and the solid was purified by dialysis against water (MWCO = 2000 Da) for 3 days to remove the catalysts. The final product was obtained as a white powder after freeze-drying (259 mg, 77%).

^{1}H NMR (DMSO-d_6, signals assigned in Fig. 2d and Fig. S4, ESI†): δ (ppm) = 8.08–7.90 (H_r), 7.40 (H_m), 7.25 (H_n), 6.65 (H_o), 5.88–5.62 (H_p and H_β), 5.27 (H_p), 4.90–4.75 (H_β), 4.60–4.40 (H_β and H_g), 3.80–3.38 (H_β), 3.35–3.23 (H_h and H_k), 2.35 (H_j), 2.05–1.90 (H_i).

Methyl-PMOXA$_{19}$-VBP (Me-19). Similar to the above description of **Alk-41**, **Me-19** was synthesized using methyl trifluoromethanesulfonate (32.13 μL, 0.47 mmol, 1 eq.) as the initiator and 2-methyl-2-oxazoline (1 g, 11.75 mmol, 25 eq.) in dry acetonitrile (3 mL). The reaction condition was adjusted to 1 h at 85 °C. The macromonomer was obtained as a colorless powder after work-up.

^{1}H NMR ($CDCl_3$, signals assigned in Fig. S5, ESI†): δ (ppm) = 7.33–7.20 (H_m, H_n, partly overlap with $CDCl_3$), 6.63 (H_o), 5.65 and 5.13 (H_p), 3.63–3.15 (H_h and H_k), 3.03–2.80 (H_s), 2.50–2.30 (H_j), 2.13–1.98 (H_i).

Synthetic and characterization data of other polymers (see Table S1 and Fig. S2–S11 (ESI†) for details).

Supramolecular hydrogel GH-40 using Ada-42 and CD-41. The Ada/β-CD functionalized PAAm hydrogel GH-40 was synthesized *via* redox initiated free radical polymerization using the **Ada-42** and **CD-41** macromonomers. Briefly, the **Ada-42** (40.97 mg, 0.01 mmol, 0.5 mol% of acrylamide) and **CD-41** (50.86 mg, 0.01 mmol, 0.5 mol% of acrylamide) macromonomers were first dissolved in 1.28 mL deionized water and treated with ultrasound for 1 min to pre-form the host–guest complex and thus the desired bismacromonomers. After that, acrylamide (150 mg,

2.11 mmol, 10 wt% of the total reaction mixture), *N*,*N*,*N*′,*N*′-tetramethylethylenediamine (1.59 μL, 0.01 mmol, 0.5 mol% of acrylamide) and *N*,*N*′-methylenebisacrylamide (1.626 mg, 0.01 mmol, 0.5 mol% of acrylamide) were added to the mixture. Then the solution was magnetically stirred and deoxygenated with argon for 10 min at 0 °C. After the addition of an aqueous solution of sodium peroxodisulfate (12.6 μL, 0.22 M, 0.5 mol% of acrylamide), the reaction mixture was transferred into a sample vial (V = 1 mL, h = 40 mm, ∅ = 8 mm), sealed and kept overnight. Finally, the hydrogels were separated from the vial and washed in deionized water for 3 days to remove impurities.

Synthetic data of other hydrogels (see Table S2 (ESI†) for details).

Instruments

Proton nuclear magnetic resonance spectroscopy (NMR). ^{1}H NMR spectra were recorded on a Bruker Avance III 500 spectrometer (500.13 MHz) using chloroform-d or DMSO-d_6 as the solvent at RT. 2D NOESY NMR spectra were obtained using D_2O as a solvent at 30 °C. All spectra were calibrated to the residual signal of the deuterated solvent.

MALDI-TOF-MS. MALDI-TOF mass spectra were obtained on an autoflex speed MALDI-TOF-/TOF–TOF system (Bruker, USA), equipped with a modified Nd:YAG laser in the positive reflector mode.

The samples were prepared in a THF solution (1 mg mL^{-1}) and dithranol (10 mg mL^{-1} in THF) was used as the matrix. Both solutions were mixed at a ratio of 1 : 1 (v/v) and spotted onto the MALDI plate. The device was calibrated prior to each measurement.

Gel permeation chromatography (GPC). GPC measurements were performed on a PL-GPC 120 (Agilent Technologies, CA), equipped with two GRAM 1000 (10 μL, 8 × 300 mm) columns under the following conditions: injection volume, 100 μL; flow rate, 1 mL min^{-1}; eluent, *N*,*N*-dimethylacetamide (DMAc) containing 5 mg mL^{-1} LiBr and 1 vol% Milli-Q water; and temperature, 70 °C. Before the measurement, the system was calibrated against polymethylmethacrylate (PMMA) standards (PSS, Mainz, Germany) in the range of 600 to 67 000 g mol^{-1}. The samples were dissolved in the above-mentioned eluent and filtered through 0.2 μm PTFE syringe filters prior to use.

Scanning electron microscopy (SEM). The formed hydrogels were analyzed using an Ultra 55 PLUS Field Emission Scanning Electron Microscope (Carl Zeiss AG, Germany) at 3 kV to study the texture of the hydrogels (magnification: 1000×). The SEM samples were freeze-dried, cut into suitable dimensions and sputter-coated with platinum before the measurement.

Fourier transform infrared spectroscopy (FT-IR). The FT-IR spectra of the macromonomers were recorded on a Vertex 80v instrument (Bruker) in the range of 4000–600 cm^{-1} with 100 scans at a resolution of 4 cm^{-1}. Analysis of the results was performed under baseline normalization and correction using OPUS 7 software (Bruker).

Dynamic light scattering (DLS). The hydrodynamic diameter of the macromonomers was recorded on a Zetasizer Nano ZS Instrument (Malvern Instruments, UK), equipped with a He–Ne laser (4 mW, λ = 633 nm) at a fixed angle of 173° (non-invasive backscatter (NIBS) mode). The results were analyzed using Zetasizer Software 7.12.

Swelling behavior of hydrogels. The swelling behavior was determined by measuring the swelling degree (Q) and swelling ratio (SR) of the hydrogel. Q was calculated using the following common formula:

$$Q = \frac{W_{\text{swollen}}}{W_{\text{dry}}}$$

where W corresponds to the weight of the gel.

The swelling ratio (SR) is described as the swelling degree of a hydrogel at the swollen state under a certain stimulus divided by the starting state, calculated using the following equation:

$$\text{SR} = \frac{Q_{\text{end point}}}{Q_{\text{starting point}}}$$

Before the measurement, hydrogels at the equilibrium state were carefully wiped using cosmetic tissues. The drying of the hydrogels was achieved by freeze-drying under vacuum.

Measurement of mechanical strength. The mechanical strength of the hydrogels was determined by rheological measurements on an ARES-G2 rheometer (TA Instruments) at RT, equipped with two stainless steel parallel plates (∅ = 25 mm). The device was calibrated and a pre-loading of the axial force at 0.1 N was set for each measurement. To determine the E-modulus of a hydrogel, a cylindrical sample (∅ = *ca.* 9 mm, h = app. 9 mm) was loaded. The compressive stress was set at a constant linear rate of 0.05 mm s^{-1}. The results were recorded until a 40% strain was obtained, and then analyzed using TRIOS software (TA Instruments).

Results and discussion

Polymer synthesis

The functionalized PMOXA macromonomers were a core part of this work and, also, the starting point. Starting from initiators bearing adamantane or alkyne groups, the corresponding PMOXA was synthesized and the reaction was terminated with **V-1** to yield PMOXA with vinylbenzyl (VBP) end groups: Ada-PMOXA$_{42}$-VBP (**Ada-42**) and alkynyl-PMOXA$_{41}$-VBP (**Alk-41**) (Scheme 1). Using β-CD-N_3, the latter was converted to β-CD-PMOXA$_{41}$-VBP (**CD-41**). Although parts of the synthesis have been reported, their combination reported here to yield Ada and β-CD end group-functionalized macromonomers is new.

The adamantane-initiator (**I-1**) was synthesized from 1-adamantanemethanol and 4-bromomethylbenzoyl bromide according to methods previously reported in the literature.[45] After two runs of column chromatography, ^{1}H NMR confirmed that the obtained **I-1** was pure enough for the next reaction step. The pure vinylating agent *N*-(4-vinylbenzyl)piperazine (4-VBP, **V-1**) bearing a polymerizable unit for radical polymerization was successfully prepared from piperazine and 4-vinylbenzyl chloride according to the methods reported in the literature.[46] All structures were confirmed by ^{1}H NMR (see Fig. S1 in the ESI† for details). A well-defined PMOXA

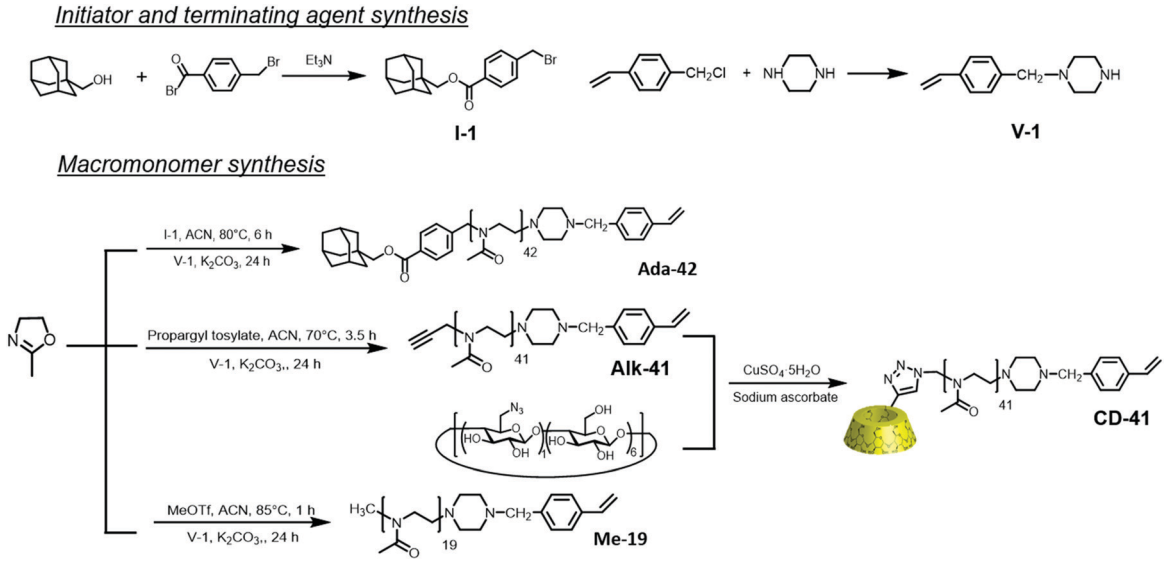

Scheme 1 Reaction sequence for the synthesis of adamantane-functionalized (**Ada-42**), alkynyl-functionalized (**Alk-41**), β-CD-functionalized (**CD-41**) and methyl-functionalized (**Me-19**) poly(2-methyl-2-oxazoline) macromonomers.

macromonomer was obtained from the LCROP of 2-methyl-2-oxazoline with a feed ratio of [monomer]:[initiator] = 40:1, using **I-1** as the initiator and **V-1** as the vinylating agent in acetonitrile at 80 °C for 8 h. Fig. 2a illustrates the NMR spectrum of the macromonomer **Ada-42**, which was purified by dialysis against MeOH. All signals characteristic of the adamantane and 4-VBP moieties could be clearly observed. The degree of polymerization (DP) of the macromonomer **Ada-42** was determined to be 42 (M_n = 4100 Da, Table 1) from the integral ratio of methylene protons from the adamantane-initiator (δ = 4.55, 2H) to those of the PMOXA backbone (δ = 3.60–3.20, 168H). This value was determined to be 44 from MALDI-TOF-MS and to be 38 from GPC (M_n = 4200 and 3600 Da, respectively) (Fig. S12, ESI† and Table 1). These results were in line with the feed ratio of the monomer to the initiator, confirming good control over molecular weight during the synthesis. Since the value from ^{1}H NMR spectroscopy relied on a direct measurement without external calibration, the obtained polymer was denoted as **Ada-42**. An end-group functionality of 98% (*i.e.* quantitative vinylization) was confirmed by ^{1}H NMR following the integration of vinyl protons (δ = 5.74 and 5.23, 2H) relative to the methylene protons of the adamantane-initiator (δ = 4.55, 2H). A large number of vinylbenzene groups were vital for the gel formation using free radical polymerization. The increase of dispersity from 1.16 to 1.18 (MALDI-TOF-MS and GPC) further confirmed a controlled polymerization. In summary, the polymerization of the adamantane macromonomer **Ada-42** was well controlled and reached a high efficiency including a high degree of vinylization.

Macromonomers with β-CD were synthesized in a similar way, but starting from propargyl *p*-toluenesulfonate as the initiator. A near quantitative vinylic functionality of 95% vinylbenzene groups was reached again for the resulting precursor **Alk-41** (Fig. 2b). A very good agreement between the number average DP determined by the ^{1}H NMR analysis (DP of 41) and the feed ratio of [monomer]:[initiator] (40:1) was observed. Control over molecular weight was confirmed by MALDI-TOF-MS and GPC analyses. Both results were close to the theoretical value predicted from the feed ratio (M_n: 3500 Da (GPC) and 4200 Da (MALDI)), and dispersity was determined to be 1.19 by GPC (Table 1).

Table 1 Synthesis data and characteristics of poly(2-methyl-2-oxazoline) macromonomers

Polymer	[Monomer]/[initiator]	$M_{n,th}$[a] [g mol^{-1}]	$M_{n,NMR}$[b] [g mol^{-1}]	$M_{n,GPC}$[c] [g mol^{-1}]	$M_{n,MALDI}$[d] [g mol^{-1}]	$Đ$[e]	End-group functionality[f] (%)
Ada-42	40	3900	4100	3600	4200	1.18	98
Alk-41	40	3600	3700	3500	4200	1.19	95
CD-41	—	4800	4900	4700	—	1.27	—
Me-19	25	2300	1900	1800	—	1.13	96
Ada-27	25	2600	2800	3100	—	1.11	90
Alk-27	25	2400	2500	2400	—	1.11	92
CD-26	—	3500	3600	2700	—	1.14	—
Ada-61	55	5200	5700	4000	—	1.17	91
Alk-58	55	4900	5200	3500	—	1.10	100
CD-59	—	6100	6500	4300	—	1.13	—

[a] Calculated from [monomer]:[initiator]. [b] Determined by end-group analysis from ^{1}H NMR spectroscopy. [c] Determined by GPC in DMAc. [d] Determined by MALDI-TOF-MS. [e] Determined by GPC and/or MALDI-TOF-MS, $Đ = M_w/M_n$. [f] Determined by end-group analysis from ^{1}H NMR spectroscopy.

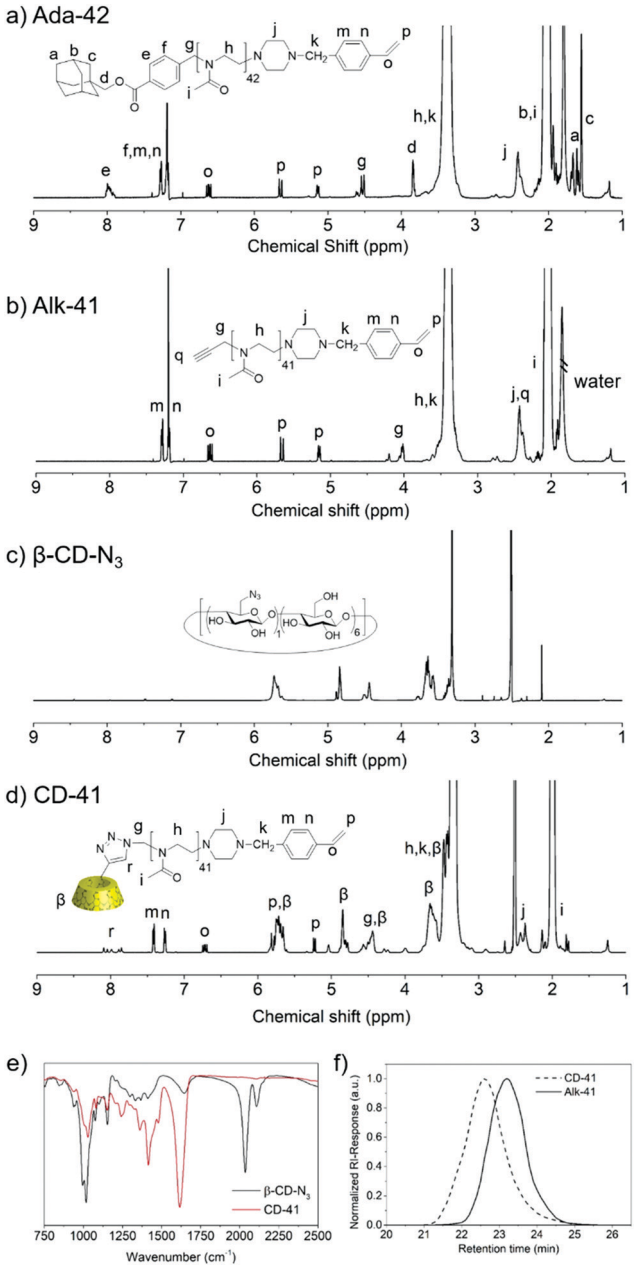

Fig. 2 ^{1}H NMR spectra of (a) **Ada-42** recorded in $CDCl_3$, (b) **Alk-41** recorded in $CDCl_3$, (c) 6-monoazido-6-monodeoxy-β-cyclodextrin recorded in DMSO-d_6, and (d) **CD-41** recorded in DMSO-d_6; (e) FT-IR spectra of **CD-41** (red line) compared with 6-monoazido-6-monodeoxy-β-cyclodextrin (black line); and (f) GPC chromatograms of **Alk-41** (solid line) and **CD-41** (dashed line).

Alk-41 was then converted into the macromonomer β-CD-PMOXA$_{41}$-VBP (**CD-41**) through copper(I)-catalyzed alkyne-azide cycloaddition (CuAAC "click" reaction)[47,48] with 6-monoazido-6-monodeoxy-β-cyclodextrin (β-CD-N_3). The resulting **CD-41** macromonomer was confirmed by ^{1}H NMR, GPC and FT-IR spectroscopy. Fig. 2d shows the ^{1}H NMR spectrum of the obtained **CD-41** macromonomer compared with pure β-CD-N_3 (Fig. 2c) and **Alk-41**. The success of click chemistry was proven by the appearance of the signal of the triazole proton at δ = 8.05 ppm and other signals corresponding to β-CD. Calculating the signal of the triazole proton and PMOXA backbone protons at 2.0 ppm gave an efficiency of the "click reaction" of approximately 80%. Comparing the FT-IR spectra (Fig. 2e and Fig. S13, ESI†) of β-CD-N_3 and **CD-41**, it became apparent that **CD-41** showed no peak for the azido group at 2107 cm^{-1}. Instead, new signals assigned to the carbonyl stretching vibration and carbon–nitrogen bond appeared at 1646 cm^{-1} and 1028 cm^{-1}, respectively. This evidence indicated the existence of the triazole ring. The GPC trace of **CD-41** showed a slight shift to the higher molecular weight compared to **Alk-41**, consistent with their added functional group (Fig. 2f). The dispersity of the polymer increased slightly (1.19 to 1.27) and M_n increased from 3.5 kDa for **Alk-41** to 4.7 kDa for **CD-41**. The combined results of ^{1}H NMR, FT-IR and GPC confirmed the successful transformation of **Alk-41** into the macromonomer **CD-41**.

All the discussed polymers have a DP of around 40. However, the chain length plays a crucial role in fine-tuning the final mechanical properties of the network. Equally important, the length of the freely mobile side chain can alter the mobility of the backbone.[49] Hence, various host/guest PMOXA macromonomers with different DPs were synthesized as well. A shorter version had a DP of around the monomer/initiator ratio of 25 (**Ada-27**, **CD-26**) and a longer version had a ratio of 60 (**Ada-61**, **CD-59**). As shown in Table 1, all $M_{n,NMR}$ and $M_{n,GPC}$ values were consistent with the theoretical ones and in line with the tendencies observed for the discussed cases of a DP of around 40. However, the overall yield of macromonomers of DP $\sim$ 25 is relatively low compared with those of DP $\sim$ 40 and DP $\sim$ 60. This discrepancy was presumably due to the lower molecular weight, which led to more loss of the product during dialysis. For all macromonomers, a relatively narrow dispersity and almost complete end-group functionality were observed. The macromonomer **Me-19**, which contains a methyl group as the end capping, was prepared as the control to determine the efficiency of the Ada/β-CD interaction. In conclusion, all PMOXA macromonomers could be prepared in a controlled manner to be used in the next steps.

Complexation studies

The networks aimed for in this study should bear a defined amount of network chains consisting of pre-formed host–guest interactions of adamantane and β-cyclodextrin, originating from the bismacromonomers. It was therefore necessary to prove the formation of the native host–guest complex of the synthesized macromonomers. We used dynamic light scattering (DLS) to investigate the size distributions of the individual macromonomers **Ada-42** and **CD-41**, and their mixture (1 : 1 eq.) in solution at 25 °C. The hydrodynamic diameter increased due to the formation of the host–guest complex between two polymer chains in the mixture (Fig. 3a). Both **Ada-42** and **CD-41** chains had small hydrodynamic diameters (2.8 and 2.2 nm, respectively) in the DMSO solution, which increased slightly in an aqueous solution (3.8 and 3.4 nm, respectively). Since PMOXA is a hydrophilic polymer, this increase is expected due

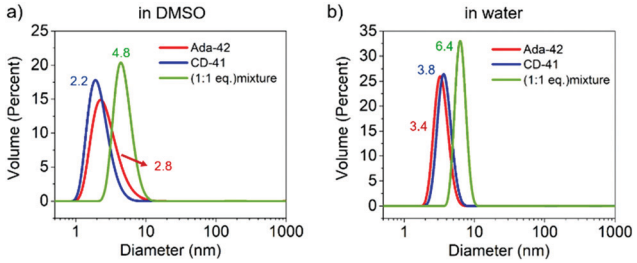

Fig. 3 Number-volume size distributions of **Ada-42**, **CD-41** and their 1 : 1 molar mixture in (a) DMSO and (b) water at RT (c = 0.2 mmol L^{-1}).

to the better solvation of the macromolecules in water. After the complex formation, the diameter increased substantially to 4.8 and 6.4 nm in DMSO and water, respectively. Connecting the single chains of DP ~ 40 *via* Ada/β-CD complexes led to an increased chain length of DP ~ 80, resulting in an increased hydrodynamic diameter. It is worth noting that the hydrodynamic diameter of the complex mixtures increased immediately after the two polymers were dissolved, demonstrating a rapid formation of the host–guest complex within seconds to minutes.

Evidence from DLS for the formation of the Ada/β-CD inclusion complex was supported by the 2D Nuclear Overhauser Effect Spectroscopy (NOESY) NMR analysis. A mixture of **Ada-42** and **CD-41** (1 : 1 eq.) was prepared in D_2O at 30 °C at 4 mmol L^{-1}. The ^{1}H NMR signals ascribed to the α and γ protons of adamantane (at 1.55 ppm and 1.65 ppm, respectively, Fig. 4) overlapped with the resonance signals corresponding to the β-CD cavity protons (H3, H5, and H6 at 3.80–3.55 ppm, Fig. 4) due to the dipolar interactions. A deep insertion of the adamantane moieties into the cavities of β-CD (*i.e.* formation of the complex) was thus confirmed, supporting the results from DLS as well as from previous ^{1}H NMR studies.[45]

Hydrogel formation and characterization

With all macromonomers in place and a proven complexation, the preparation of the Ada/β-CD supramolecular hydrogels using host–guest functionalized bismacromonomers was the next step (schematically illustrated in Fig. 5a). Prior to the radical copolymerization, both hydrophilic PMOXA macromonomers were dissolved in water treated with ultrasound for 1 min to pre-form the host–guest complex and thus the desired bismacromonomers. Hydrogels were prepared by FRP using acrylamide (AAm) as the backbone, *N*,*N*′-methylenebis-(acrylamide) (BIS, 0.5 mol%) as the covalent cross-linker, the bismacromonomer (0.5 mol%) as the non-covalent cross-linker, sodium persulfate (NaPS) as the initiator and *N*,*N*,*N*′,*N*′-tetramethylethylenediamine (TMEDA) as the accelerator in water. Hence 1.0 mol% was added in total, half of which is the bismacromonomer in a 1 : 1 (CD : Ada) ratio. Four kinds of double cross-linked hydrogels were prepared, all differing in the PMOXA length in the bismacromonomer. The hydrogel GH-25 contained bismacromonomers from **Ada-27** and **CD-27**, leading to DP ~ 50 in the PMOXA bismacromonomer. The hydrogels GH-40 and GH-60 contained macromonomers with DP ~ 80 (**Ada-42** + **CD-41**) and DP ~ 120 (**Ada-61** + **CD-59**), respectively. The fourth one was a graft hydrogel based on **Me-19** and named GH-19Me, containing no Ada/β-CD complexes. In addition, the pure PAAm hydrogel (named H-AAm) was also synthesized as the additional control hydrogel besides the hydrogel GH-19Me. Homogeneous and transparent hydrogels were obtained after washing in deionized water for 3 days. Since the Ada/β-CD functionalized bismacromonomer was pre-formed, the hydrogels GH-25, GH-40, and GH-60 contained the corresponding supramolecular PMOXA network chains already after their synthesis. To understand the swelling and mechanical properties of double cross-linked supramolecular hydrogels GH-25, GH-40 and GH-60 compared to GH-19Me and H-AAm, all synthesized hydrogels were prepared by the use of the same amount of the BIS cross-linker (0.5 mol%). All double cross-linked hydrogels contained the same amount of bismacromonomer as the second cross-linker (0.5 mol%). The additional cross-linkers affected the swelling degrees (Q) of all double cross-linked hydrogels GH-25, GH-40 and GH-60 (Fig. 5c). Compared to H-AAm, GH-19Me presented a higher swelling degree of ~21 rather than the value of ~18. This is mainly due to the unconnected, hydrophilic PMOXA side chains, which increased the hydrophilicity of the hydrogel. In particular, when compared to the graft control hydrogel GH-19Me, the double cross-linked hydrogels exhibited a considerably lower Q value of ~16 for GH-25 and GH-40, followed by GH-60 (Q ~ 17). The slightly higher Q value of GH-60 is easily explained by the longer PMOXA chains, although not as high as expected for this loosely cross-linking

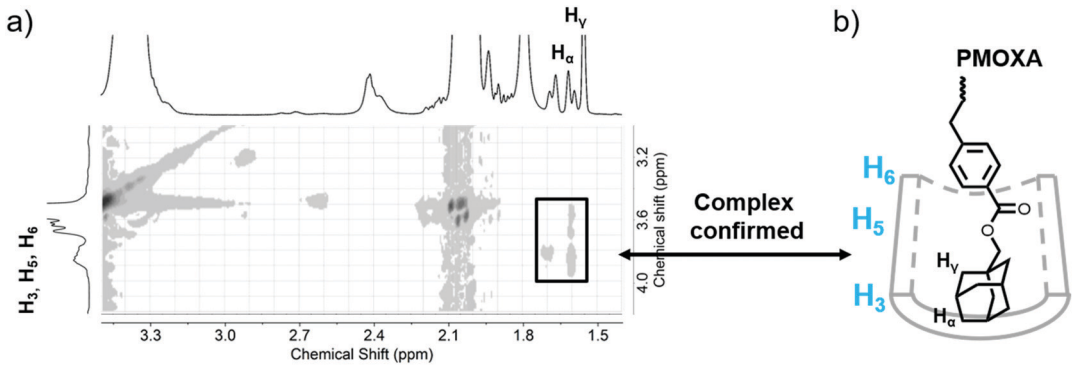

Fig. 4 (a) 2D NOESY spectrum of a 1 : 1 molar mixture of **Ada-42** and **CD-41** (both 4 mmol L^{-1}) in D_2O at 30 °C and (b) schematic representation of the detected insertion mode in the host–guest complex between the adamantane containing end group of **Ada-42** and **CD-41**.

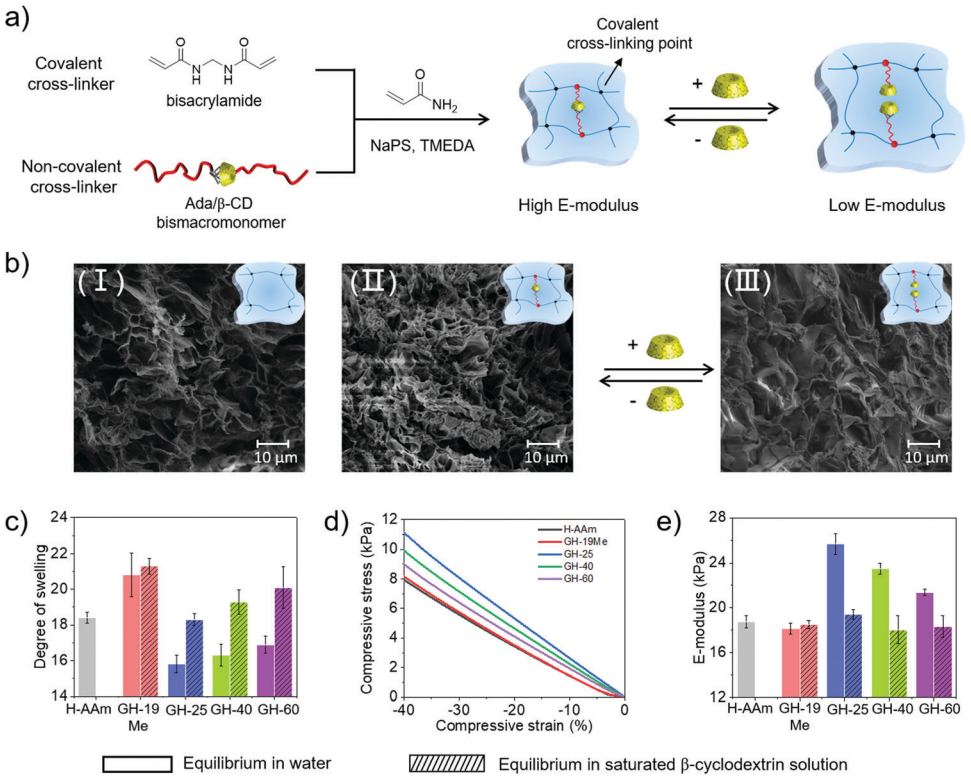

Fig. 5 (a) Preparation and chemical structure of Ada/β-CD supramolecular hydrogels using host–guest functionalized bismacromonomers. The formed hydrogel showed a change of E-modulus in response to free β-CD molecules in aqueous solution. (b) Scanning electron microscopy image of the hydrogels (I) H-AAm, (II) GH-25 and (III) GH-25 after adding free β-CD. (c) Swelling degree of the synthesized hydrogels. (d) Compressive stress (up to 40% strain) and (e) E-modulus (measured up to 20% strain from the stress–strain curves) of different hydrogels at the equilibrium state in water and in the saturated β-CD solution.

bismacromonomer. However, the overall lower Q demonstrated the stability of the Ada/β-CD complexes in the network as they firmly suppressed the swelling ability of the hydrogels.

The Ada/β-CD host–guest interaction could undergo a reversible association and dissociation by introducing a competitive host or guest group. After adding free β-CD as competitive host molecules to break the complex, the swelling of the hydrogels was tested again. All graft and double cross-linked hydrogel samples (cylinder-shaped, diameter of approximately 4 mm, height of approximately 10 mm, equilibrium in water) were immersed in 10 mL of saturated β-CD aqueous solutions for 24 h. As shown in Fig. 5c and Table 2, the swelling degree of the host–guest hydrogels GH-25, GH-40 and GH-60 increased to ∼18, ∼19 and ∼20, respectively, whereas that of GH-19Me remained constant. All double cross-linked hydrogels now showed a swelling behavior in the range of GH-19Me and H-AAM. The competitive β-CD units hence showed high affinity for the adamantane groups, resulting in a dissociation of the supramolecular bonds in the PMOXA network chains (Fig. 5a). Broken chains meant a lower network density and that the introduced bismacromonomers no longer acted as additional cross-linking points. This immediately decreased the cross-linking density of the networks containing Ada/β-CD host–guest complexes. Both effects consequently explained the additional swelling of the double cross-linked hydrogels GH-25, GH-40 and GH-60.

The interior morphologies of the H-AAm and GH-25 hydrogels were investigated by SEM. The H-AAm hydrogels exhibited well-defined porous interior structures with pore sizes in the range of single digits to tens of micrometers after freeze-drying (Fig. 5b). The double cross-linked hydrogel GH-25, on the other hand, presented distinctly smaller pore sizes (∼1–5 μm) due to the introduction of the bismacromonomer (= more cross-linking points). After treating the GH-25 hydrogel with free β-CD moieties, their SEM image was similar to that of the H-AAm gels. The pore size increased, and the pore density decreased, as the hydrogel was treated with β-CD moieties. This observation demonstrated that the β-CD units on the network chains were successfully replaced by the free β-CD moieties, resulting in a dissociation of the host–guest complexation. As soon as the Ada/β-CD complexes were replaced, the PMOXA chains were no longer part of the network structure but just dangling graft chains. Although some complexes may have still been in place, the underlying acrylamide network frame governed the hydrogel properties, leading to a structure very similar to H-AAm.

As the host–guest complexation clearly influenced the swelling behaviour and network structure, its influence on the mechanical behaviour of the double cross-linked hydrogels, the Young's modulus of the hydrogel samples, was then investigated. For this purpose, the compression analysis until 40% strain was performed using cylindrical samples ($\varnothing$ = *ca.* 9 mm, h = app. 9 mm) of the prepared hydrogels (Fig. 5d and e and Table 2).

Table 2 Synthesis data and characteristics of (graft) poly(acrylamide) hydrogels

	Graft polymer chains					
Hydrogel[a]	Guest	Host	Q_w[b]	Q_{CD}[c]	E_w[d] (kPa)	E_{CD}[e] (kPa)
H-AAm	—	—	18 ± 0.3	—	18.77 ± 0.55	—
GH-19Me	**Me-19**		21 ± 1.2	21 ± 0.4	18.13 ± 0.49	18.50 ± 0.36
GH-25	**Ada-27**	**CD-26**	16 ± 0.5	18 ± 0.3	25.66 ± 0.93	19.44 ± 0.43
GH-40	**Ada-42**	**CD-41**	16 ± 0.6	19 ± 0.7	23.48 ± 0.49	18.04 ± 1.26
GH-60	**Ada-61**	**CD-59**	17 ± 0.5	20 ± 1.1	21.38 ± 0.3	18.33 ± 0.97

[a] Synthesis conditions: 10 wt% monomer, 0.5 mol% of each macromonomer, 0.5 mol% cross-linker, 0.5 mol% initiator, 0.5 mol% accelerator, solvent:water. [b] Degree of swelling in water at equilibrium. [c] Degree of swelling in saturated β-CD aqueous solutions at equilibrium. [d] E-modulus determined by rheology. [e] E-modulus after reaction with competitive β-CD units, determined by rheology.

The compressive stress of all samples increased strictly linearly within the first 20% strain, indicating defect-free gels.

The analysis of the elastic modulus revealed that both H-AAm and GH-19Me hydrogels had similar elastic modulus values of about 18 kPa. All double cross-linked hydrogels with host–guest interactions, GH-25, GH-40 and GH-60, showed significantly increased elastic moduli. As already discussed, the host–guest complex results in a denser network with more network chains and network joints, which perfectly explains these results. Moreover, the additional mechanical strength of the host–guest hydrogels was highly tunable through the modulation of the molecular weight of PMOXA chains. Compared with the value of 18.13 kPa for GH-19Me, the E-modulus of GH-25 presented an approximately 36% amplification to 25.6 kPa. In the cases of GH-40 and GH-60, an increase in mechanical strength was observed with the E-moduli of 23.4 kPa and 21.3 kPa, respectively. The additional mobility introduced by longer PMOXA chains, *i.e.* a less dense network structure, decreased mechanical toughening for the same reason as it increased the degree of swelling discussed earlier. It should be noted that the mechanical properties of the hydrogel were significantly enhanced through the largely increased theoretically available cross-linking points in double cross-linked hydrogels compared to H-AAm (see above). Similar to the swelling experiments, all Ada/β-CD hydrogels were then immersed in aqueous β-CD solutions for 24 h to break the Ada/β-CD complexes in the PMOXA network chains, including GH-19Me as the control hydrogel. Then, elastic moduli were immediately re-measured. Free β-CD units indeed broke the host–guest complex in the network chains of PMOXA (Fig. 5a), leading to a sharp decrease in the E-moduli of all hydrogels with Ada/β-CD complexes down to ~18–19 kPa. These lower values were almost the same as those of the pure PAAm gel H-AAm and also of GH-19Me, suggesting that no or only a low number of complexes were still present. As expected, the E-modulus of GH-19Me did not change after exposure to free β-CD moieties. This result nicely underlined that the additional mechanical strength just discussed indeed originated from the different network structure due to the Ada/β-CD host–guest interactions in the graft hydrogels. By breaking the complex, the PMOXA network chains no longer connected two different acrylamide chains, explaining all macroscopic changes just mentioned. Importantly, the change in the cross-linking density was also consistent with the results of morphology measurements. The additional mechanical strength of the hydrogels could even be related to the chain length of the used bismacromonomer. Altogether, the swelling behavior, mechanical properties and interior structures of the double cross-linked supramolecular hydrogels were well controlled by the association and dissociation of the host–guest complexation in the PMOXA network chains.

Conclusions

We designed and prepared novel double cross-linked supramolecular hydrogels based on the host–guest interactions of adamantane and β-cyclodextrin taking advantage of the strength of this bond in defined additional network chains. These hydrogels had permanent network points, but also an equal amount of non-permanent cross-linker links held together by the host–guest interactions. Well-defined hydrophilic poly(2-methyl-2-oxazoline) macromonomers bearing either pendent adamantane groups (Ada–PMOXA) or β-cyclodextrin moieties (β-CD–PMOXA) have been synthesized, which were clearly verified by the ^{1}H NMR, MALDI-TOF-MS and GPC analyses. The 2D NOESY NMR and DLS measurements provided unambiguous evidence for the host–guest interaction, *i.e.* for the *in situ* formation of the bismacromonomers from a 1 : 1 mixture of two macromonomers. The resulting double cross-linked supramolecular hydrogel systems showed the desired reduced swelling behaviour and increased mechanical strength in comparison to hydrogels with no host–guest interactions. Stable supramolecular non-covalent interactions between complementary functionalized PMOXA chain segments were thus proven as the resulting PMOXA chains contributed to the network. It is important to note that our supramolecular interactions significantly enhanced the mechanical strength. After adding additional β-CD moieties, the host–guest complex within the PMOXA chains broke, and only the cross-linking points of BIS contributed to the elastic properties of the hydrogels. The PMOXA chains then acted as dangling graft side chains in the hydrogels. Extensively different from previous studies, this work demonstrates that the swelling behaviour and mechanical strength of such double cross-linked hydrogels could be easily tailored by changing the molecular weight of host–guest conjugated PMOXA chains in the bismacromonomers. Initial insights into the elastic properties of this kind of hydrogel will serve as a basis for future studies.

The controlling property of the host–guest graft hydrogels could have a promising role to play in hydrogels as chemical sensors and actuators in microfluidic setups, and also within sophisticated drug delivery systems.

Conflicts of interest

The authors declare no conflicts of interest.

Acknowledgements

The authors gratefully acknowledge the financial support by Deutsche Forschungsgemeinschaft (Graduiertenkolleg ''Hydrogelbasierte Mikrosysteme'', DFG-GRK 1865). Y. C. thanks Maria Auf der Landwehr, Dr. Karin Sahre, Dr. Hartmut Komber and Mikhail Malanin for the SEM, MALDI-TOF-MS, 2D NOESY NMR and FT-IR measurements, respectively.

References

1 C. Bastiancich, P. Danhier, V. Preat and F. Danhier, *J. Controlled Release*, 2016, **243**, 29.
2 J. Li and D. J. Mooney, *Nat. Rev. Mater.*, 2016, **1**, 16071.
3 H. Wang and S. C. Heilshorn, *Adv. Mater.*, 2015, **27**, 3717.
4 N. A. Peppas and D. S. Van Blarcom, *J. Controlled Release*, 2016, **240**, 142.
5 J. Erfkamp, M. Guenther and G. Gerlach, *Sensors*, 2019, **19**, 2858.
6 K. Miyamae, M. Nakahata, Y. Takashima and A. Harada, *Angew. Chem., Int. Ed.*, 2015, **54**, 8984.
7 C. Ma, W. Lu, X. Yang, J. He, X. Le, L. Wang, J. Zhang, M. J. Serpe, Y. Huang and T. Chen, *Adv. Funct. Mater.*, 2018, **28**, 1704568.
8 M. Guo, L. M. Pitet, H. M. Wyss, M. Vos, P. Y. Dankers and E. W. Meijer, *J. Am. Chem. Soc.*, 2014, **136**, 6969.
9 Z. Feng, H. Zuo, W. Gao, N. Ning, M. Tian and L. Zhang, *Macromol. Rapid Commun.*, 2018, **39**, e1800138.
10 S. Burattini, B. W. Greenland, D. H. Merino, W. Weng, J. Seppala, M. C. Howard, W. Hayes, M. E. Mackay, I. W. Hamley and S. J. Rowan, *J. Am. Chem. Soc.*, 2010, **132**, 12051.
11 Q. Wang, J. L. Mynar, M. Yoshida, E. Lee, M. Lee, K. Okuro, K. Kinbara and T. Aida, *Nature*, 2010, **463**, 339.
12 X. Le, W. Lu, J. Zheng, D. Tong, N. Zhao, C. Ma, H. Xiao, J. Zhang, Y. Huang and T. Chen, *Chem. Sci.*, 2016, **7**, 6715.
13 D. C. Tuncaboylu, M. Sari, W. Oppermann and O. Okay, *Macromolecules*, 2011, **44**, 4997.
14 G. Yu, K. Jie and F. Huang, *Chem. Rev.*, 2015, **115**, 7240.
15 M. Miyauchi and A. Harada, *J. Am. Chem. Soc.*, 2004, **126**, 11418.
16 B. Schmidt and C. Barner-Kowollik, *Angew. Chem., Int. Ed.*, 2017, **56**, 8350.
17 M. V. Rekharsky and Y. Inoue, *Chem. Rev.*, 1998, **98**, 1875.
18 R. Pinalli, G. Brancatelli, A. Pedrini, D. Menozzi, D. Hernandez, P. Ballester, S. Geremia and E. Dalcanale, *J. Am. Chem. Soc.*, 2016, **138**, 8569.
19 L. Moreira, B. M. Illescas and N. Martin, *J. Org. Chem.*, 2017, **82**, 3347.
20 H. Qian, D.-S. Guo and Y. Liu, *Asian J. Org. Chem.*, 2012, **1**, 155.
21 Y. Yang, X. L. Ni, J. F. Xu and X. Zhang, *Chem. Commun.*, 2019, **55**, 13836.
22 M. A. Rajora, J. W. H. Lou and G. Zheng, *Chem. Soc. Rev.*, 2017, **46**, 6433.
23 G. Chen and M. Jiang, *Chem. Soc. Rev.*, 2011, **40**, 2254.
24 J. Szejtli, *Chem. Rev.*, 1998, **98**, 1743.
25 C. Koopmans and H. Ritter, *Macromolecules*, 2008, **41**, 7418.
26 Y. Takashima, S. Hatanaka, M. Otsubo, M. Nakahata, T. Kakuta, A. Hashidzume, H. Yamaguchi and A. Harada, *Nat. Commun.*, 2012, **3**, 1270.
27 M. Nakahata, Y. Takashima, H. Yamaguchi and A. Harada, *Nat. Commun.*, 2011, **2**, 511.
28 T. Sun, Y. Li, H. Zhang, J. Li, F. Xin, L. Kong and A. Hao, *Colloids Surf., A*, 2011, **375**, 87.
29 M. R. Eftink, M. L. Andy, K. Bystrom, H. D. Perlmutter and D. S. Kristol, *J. Am. Chem. Soc.*, 1989, **111**, 6765.
30 X. Chen, C. Dong, K. Wei, Y. Yao, Q. Feng, K. Zhang, F. Han, A. F.-T. Mak, B. Li and L. Bian, *NPG Asia Mater.*, 2018, **10**, 788.
31 T. Cai, S. Huo, T. Wang, W. Sun and Z. Tong, *Carbohydr. Polym.*, 2018, **193**, 54.
32 M. Zhang, D. Xu, X. Yan, J. Chen, S. Dong, B. Zheng and F. Huang, *Angew. Chem., Int. Ed.*, 2012, **51**, 7011.
33 Y.-G. Jia and X. X. Zhu, *Chem. Mater.*, 2014, **27**, 387.
34 J. Sheng, Y. Wang, L. Xiong, Q. Luo, X. Li, Z. Shen and W. Zhu, *Polym. Chem.*, 2017, **8**, 1680.
35 T. Kakuta, Y. Takashima, M. Nakahata, M. Otsubo, H. Yamaguchi and A. Harada, *Adv. Mater.*, 2013, **25**, 2849.
36 C. B. Rodell, N. N. Dusaj, C. B. Highley and J. A. Burdick, *Adv. Mater.*, 2016, **28**, 8419.
37 Z. Wang, Y. Ren, Y. Zhu, L. Hao, Y. Chen, G. An, H. Wu, X. Shi and C. Mao, *Angew. Chem., Int. Ed.*, 2018, **57**, 9008.
38 Y. Che, S. Zschoche, F. Obst, D. Appelhans and B. Voit, *Polym. Chem.*, 2019, **57**, 2590.
39 R. Luxenhofer, G. Sahay, A. Schulz, D. Alakhova, T. K. Bronich, R. Jordan and A. V. Kabanov, *J. Controlled Release*, 2011, **153**, 73.
40 T. X. Viegas, M. D. Bentley, J. M. Harris, Z. Fang, K. Yoon, B. Dizman, R. Weimer, A. Mero, G. Pasut and F. M. Veronese, *Bioconjugate Chem.*, 2011, **22**, 976.
41 M. Glassner, M. Vergaelen and R. Hoogenboom, *Polym. Int.*, 2018, **67**, 32.
42 F. C. Gaertner, R. Luxenhofer, B. Blechert, R. Jordan and M. Essler, *J. Controlled Release*, 2007, **119**, 291.
43 K. Aoi and M. Okada, *Prog. Polym. Sci.*, 1996, **21**, 151.
44 N. Adams and U. S. Schubert, *Adv. Drug Delivery Rev.*, 2007, **59**, 1504.
45 J. Stadermann, H. Komber, M. Erber, F. Däbritz, H. Ritter and B. Voit, *Macromolecules*, 2011, **44**, 3250.
46 A. Gross, G. Maiel and O. Nuyken, *Macromol. Chem. Phys.*, 1996, **197**, 2811.
47 J. E. Hein and V. V. Fokin, *Chem. Soc. Rev.*, 2010, **39**, 1302.
48 L. Liang and D. Astruc, *Coord. Chem. Rev.*, 2011, **255**, 2933.
49 Y. Kaneko, K. Sakai, A. Kikuchi, R. Yoshida, Y. Sakurai and T. Okano, *Macromolecules*, 1995, **28**, 7717.

